Spectrum of Engineering Sciences
ISSN (e) 3007-3138 (p) 3007-312X
Volume 4, Issue 2, 2026

FACILE SYNTHESIS OF FLEXIBLE REDUCED GRAPHENE OXIDE–LARGE SIZE COPPER NANOWIRES (RGO/CU LNWS) COMPOSITE FILM WITH PROMISING ELECTRICAL CONDUCTIVITY PERFORMANCE

[*1]Shah Nawaz Phulpoto, [2]Zubeda Bhatti, [3]Nadir Ali Rind, [4]Gada Hussain, [5]Shahid Raza, [*6]Ashique Hussain Jatoi

[1]Department of Physics, Shaheed Benazir Bhutto University Benazir Abad Sindh.
[2]Department of Physics, Shah Abdul Latif University Khairpur Sindh.
[3]Department of Molecular Biology & Genetics, Shaheed Benazir Bhutto University Benazir Abad Sindh.
[4]Department of Physics, Shaheed Benazir Bhutto University Benazir Abad Sindh
[5]Institute of Physics, University of Sindh Jamshoro
*[*6]Department of Chemistry, Shaheed Benazir Bhutto University Benazir Abad Sindh.*
*[*1]shahnawaz.phulpoto@sbbusba.edu.pk*

DOI:

Keywords
Graphene, Graphene oxide, Nanowires

Article History
Received on: 04 Jan 2026
Accepted on : 08 Feb 2026
Published on: 09 Feb 2026

Corresponding Author:
Shah Nawaz Phulpoto
Ashique Hussain Jatoi

Abstract
A new strategy is reported to fabricate free stand Reduced Graphene oxide sheets using small and large-size Copper Nanowires (CU SNWs and CU LNWs) with rGO film as an over-coating protective layer. The results show that ultrathin rGO micro sheets provide the best combination of a protective effect and electrical properties on CU LNWs networks and thus could enable the design of high-performance electrical conductivity which as-made rGO/CU LNWs film. The electrical conductivity of rGO/CU LNWs composites was significantly improved compared to rGO/CU SNws, CU and rGO alone. Moreover, the conducting path between rGO and CU LNWs formed because the structural defects in rGO were effectively repaired by decoration with CU LNWs. Our results may pave the way for a new promising rGO/ CU LNWs hybrid film applications.

INTRODUCTION

Graphene research was originally motivated by its peculiar electrical transport properties and the promise of future applications in Nano electronics.[1],[2] [2b] Graphene sheets, owing to their exceptional thermal and mechanical properties and high electrical conductivity, are also of great interest to serve as new nanoscale building blocks to create unique macroscopic materials.[3],[4] [5] Recent studies have shown that graphene film can be prepared in large quantities through chemical conversion from graphite,[6] [6] [6a] [7] [8] which has facilitated the fabrication of graphene-based electronic devices [9] [10] and has also made it possible to create new bulk materials comprising graphene sheets for a broader range of applications.[9-11] Graphene dispersions were prepared by controlled reduction of GO dispersions with hydrazine using the procedure reported in one of our publications.[12] [13] Graphene paper was then fabricated by filtration of a measured amount of graphene dispersion through an Anodisc membrane filter, followed by air-drying and peeling from the filter. The samples of graphene paper were annealed at different temperatures before being cooled to room temperature for various measurements.

*CONTACT: shahnawaz.phulpoto@sbbusba.edu.pk Department of Physics, Shaheed Benazir Bhutto University, Benazir Abad Sindh Pakistan

We observe that as-prepared graphene paper displays a shiny metallic lustre on both sides (Fig. 2A). Scanning electron microscopy (SEM) analysis reveals that the surface of the graphene paper is relatively smooth (Fig. 2B), and the fracture edges of the paper exhibit a layered structure throughout the entire cross-section (Fig. 2A). These results indicate that, identical to hydrophilic GO sheets, [14] chemically reduced graphene sheets can also be assembled to form highly ordered microscopic structures under vacuum filtration. The thickness of the graphene paper can be varied from 10-15 nm by adjusting the volume of the colloidal dispersion. Nevertheless, only stable and agglomerate- free graphene colloids can produce uniform, smooth, and shiny paper. In contrast to GO paper, [14] graphene film cannot be re-dispersed into the water by ultra-sonication, exhibiting excellent water-resistance behavior. After the pioneering work of graphene, there have been a lot of efforts to investigate a chemical route to produce exfoliated graphene oxide (GO) and reduced graphene oxide (rGO).[15]. The chemical approach for producing GO and rGO is suited for a mass production process and a low-cost procedure. It can especially render us a large variety of different variants of graphene with chemical modifications. Several fabrication methods for Cu NWs have been developed, such as electrospinning,[16] [17] electrochemical depositions,[18] templates or membrane method,[19] and reverse micelle system.[20] However, the above methods are generally not applicable because of the limitation in mass production and process complexity.[21] The newly developed chemical reduction method in aqueous solution has drawn much attention since it is facile and low cost [18, 22] [11, 22-23],[23] This technique mainly relies on reducing Cu LNWS in an aqueous solution with the help of a reducing agent (hydrazine hydrate) and a capping agent like Ethylanadiomine.[24] However, the procedure often produces nanowires with bad dispersion and is easy to be oxidised.[25]

In this work, a large-scale synthesis procedure for Cu LNWs was developed we done. Well dispersed single-crystalline Cu LNWs with large aspect ratios were successfully synthesised through the facile aqueous reduction route at low temperatures. Our research developed a large-scale synthesis procedure for Cu LNWs with Well-disposed single-crystalline synthesised by the solvothermal method. The reduced graphene oxide (rGO) film constructs rGO/CU SNws and rGO/CU LNws hybrid film architecture. The rGO/CU LNws have unique architecture that can provide a high electrical conductivity of the overall film based on the well-interacted CU LNWs and rGO film. By controlling the surface chemistry, reduced graphene oxide (rGO) is wrapped onto the Cu LNWs surface to form a uniform distribution with a thickness of around 10-15 nm. To the best of our knowledge, this is the first time to use ultra-long Cu LNWs as Electrical conductive fillers with reduced graphene oxide to achieve high electrical conductivity.

EXPERIMENTAL SECTION

Synthesis of CU LNws

Preparation of Cu LNWs. Herein, we demonstrate that those high-quality ultralong copper nanowires[26] [27] [28] (all free-standing: 70-90 nm in diameter, 40-60 nm in length can be synthesised on a large scale with a facile aqueous reduction route at low temperatures.[29] In each synthesis, 20-30 mL of NaOH (3.5-15 M) and 0.5-1.0 mL of Cu (NO3)2 (0.10 M) aqueous solution were added to a glass reactor (capacity 50 mL). Varying amounts of ethylenediamine (EDA; 0.050-2.0 mL; 99 wt %) and hydrazine (0.020-1.0 mL; 35 wt %) were also added sequentially, followed by thorough mixing of all reagents. The reactor was then placed in a water bath with temperature control over 20-90 °C (optimized at 60 °C) for 15 min to 1 h; copper products were

washed and harvested with centrifugation-re-dispersion cycles. The final products were then kept in a water-hydrazine solution at room temperature. Both large-size and small-size CU Nanowires (denoted as CU LNws and CU SNws) were prepared from Copper Nanowires. We also found that the above ultra-long Cu LNWs could break into short ones SCu NWs (<20 μm) through sonication.

Synthesis of Graphene Oxide (GO) and rGO

GO was synthesized from natural graphite powders via a modified Hummer's method [12 30] . The GO was thoroughly purified by washing cycles with deionized (DI) water and centrifuging. The GO hydrogel was finally obtained by decanting the supernatant after centrifuging. The concentration of the GO hydrogel was determined by drying a portion of the GO hydrogel in a vacuum oven at 50 °C overnight. A GO suspension (3mgml^{-1}) was prepared by diluting the GO hydrogel with DI water. GO hydrogel was obtained after the pH value of the supernatant was close to 6. rGO was produced from the GO (25.0 mL, 0.05 wt %) and was mixed with 25.0 mL of water and 11.0 μL of hydrazine solution (80 wt %) in a glass vial. After vigorously shaken or stirred for a few minutes, the vial was put in a water bath (60 C) for one h.

Preparation of rGO/CU LNWs Composites

0.1 ml of an aqueous suspension of rGO sheets were mixed evenly with 0.2 ml of an aqueous suspension of CU NWs (0.5 mg ml^{-1}). For the fabrication of neat rGO/CU, rGO/CU SNWs, and rGO/CU LNws films, the aqueous dispersed rGOs (50 mg) were prepared by a vacuum filtration method using a Millipore filter (50mm in diameter and 0.45 lm in pore size). and dried (50 C, 5 min) was used to produce graphene films in free stand. To the best of our knowledge, this is the first time to use LCuNWs for the electrical conductivity and achieve the high electrical conductivity.

CHARACTERISATION

The surface morphologies of the films were carried out by scanning electron microscopy (SEM). The reduction of GO, rGO, rGO/CU SNWs and rGO/CU LNws in hybrid films was testified using X-ray diffraction, Fourier transforms infrared (FTIR spectrometer), and Raman spectra. And also GO and rGO content was determined through Thermogravimetric analysis (TGA). The electrical resistivity of the films was measured by using the Conductivity meter. We demonstrate a solution-based method to produce high-quality ultrathin copper reduced-graphene-oxide nanowires. By controlling the surface chemistry, graphene oxide (GO) film are wrapped onto the Cu NWs surface to form a uniform coating with a thickness of around 1-15 nm. The rGO/CU LNWs are highly stable in various polar solvents stored in air. We fabricated transparent conducting films using the rGO/CU LNWs colloidal suspensions that show excellent conductivity and significantly improved resistance toward oxidation.

RESULTS & DISCUSSIONS

Scanning Electron Microscope (SEM):

Figure 1C and 1D shows the Cu NWs with an average diameter of 10-15 μm were synthesised. We observe that as-prepared reduced graphene oxide (rGO) paper displays a shiny metallic lustre on both sides (Fig. 2A). Scanning electron microscopy (SEM) analysis reveals that the surface of the reduced graphene oxide (rGO) paper is relatively smooth (Fig. 2C), and the fracture edges of the papers exhibit a layered structure throughout the entire cross-section (Fig. 2A), which looks similar to the microstructure obtained for GO paper prepared using the same method.[31] [30]These results indicate that similar to hydrophilic GO sheets,[31] chemically reduced graphene sheets can also be assembled to form highly ordered microscopic structures under vacuum filtration-induced directional flow. The thickness of the reduced graphene oxide paper can be varied from tens of nanometers to around 10-15 nm by adjusting the volume of the colloidal dispersion. Nevertheless, only stable and agglomerate-free graphene colloids can produce uniform, smooth, and shiny paper. In contrast, to GO paper,[32] [33] reduced graphene oxide paper cannot be re-dispersed into the water by ultra-sonication, exhibiting excellent water-resistance behavior. A highly aligned structure can be assembled in a reduced Graphene sheet, as evidenced by SEM images shown in Figure 2A. Graphene sheets overlap horizontally and stack up to form a layer-by-layer structure in the vertical direction.

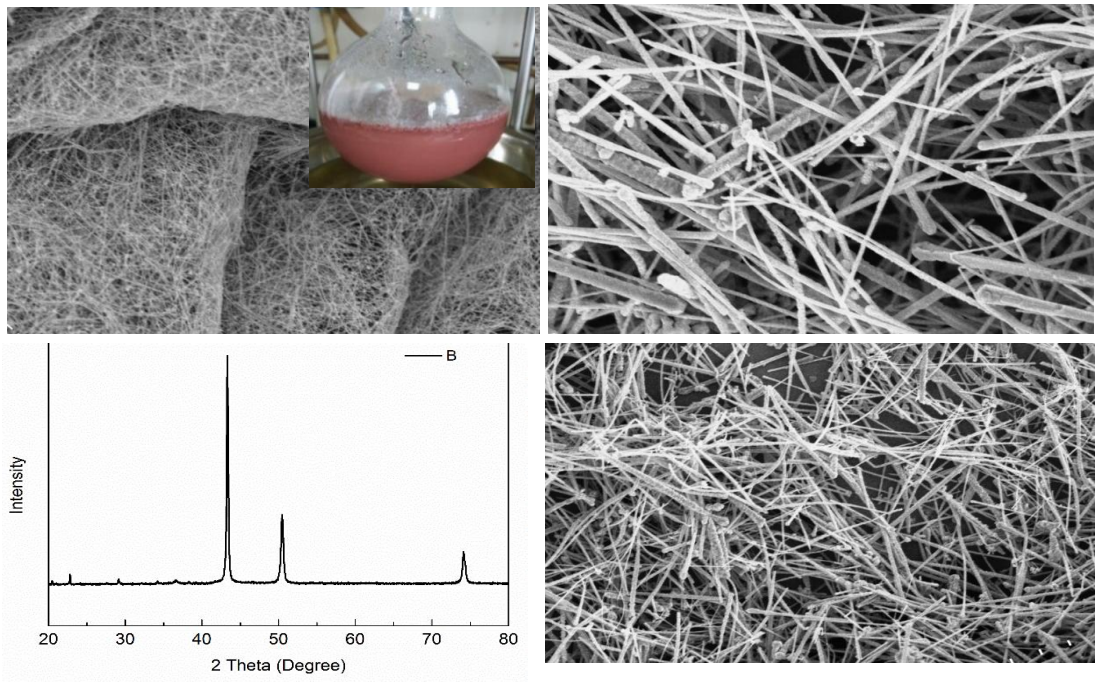

Fig. 1 – (a) Low- and (b) XRD pattern of Cu LNWs, high-magnification SEM images of as-synthesized Cu LNWs, (c) SEM images of as-synthesized Cu LNWs, and (d) SEM image of Cu SNWs. Inset of (a) is the photograph of aqueous suspension of Cu LNWs,

As shown in these images, the prepared nanowires are straight (Figure 1A, C and D), with constant diameters in the range of 60-160 nm (mostly in 90-120 nm). The wires are ultralong, having lengths of more than 40 nm, our experiments indicate that a high concentration of NaOH is essential to prevent the copper ions from forming copper hydroxide precipitates. On the other hand, a certain amount of EDA is also indispensable to control product morphology. The high concentration of NaOH, the needed amount of EDA is small, while for a lower concentration of NaOH, the amount of EDA has to be increased accordingly in order to obtain high regularity for the 1D product

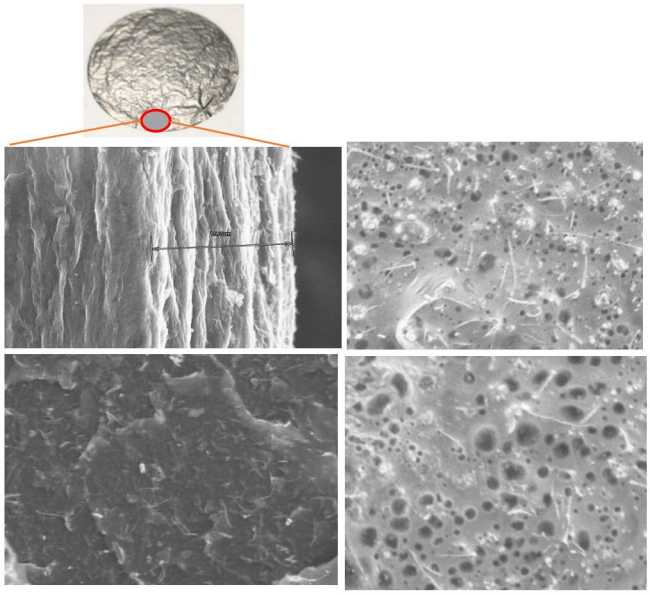

Fig. 2 – (a) Cross-sectional SEM images of (rGO/Cu LNWs) film with free stand film. (b) Scanning electron microscope (SEM) images of rGO/CU LNWS (c) SEM image of reduced Graphene oxide (rGO) thin film and (d) SEM image of rGO/Cu SNWs films.

X-rays diffraction (XRD)

The XRD pattern of natural graphite reveals the characteristic intense diffraction peak of graphite at 2θ = 26.4° (Fig 3A), which corresponds to the graphene interlayer of (002) with the d spacing of 0.34 nm.[34 35] The disappearance of the characteristic graphite peak at 26.4° and the formation of a broad peak at 9.7° of dried GO indicate the intercalation of hydroxyl, carbonyl, and epoxide groups in graphite interlayer during the chemical oxidation process.[12 36 37] Abundant amounts of those functional groups on the surface of GO were removed and simultaneously leading to a fast exfoliation after the reduction to obtain rGO. The absence of a significant diffraction peak in the XRD Notes that the d-spacing of the resulting reduced graphene oxide (GO) paper is slightly greater than, but quite close to, that of graphene layers in pristine natural graphite, indicating that chemically prepared graphene sheets are similar to the pristine sheets. The slightly increased d-spacing of chemically prepared graphene paper can be ascribed to the presence of a small amount of residual oxygen-containing functional groups or other structural defects. After Hydrazine hydrate reduction, the peak of Graphene Oxide at 8.92 disappeared. This meant that many oxidized functional groups were removed from the interlayer spacing of Graphene Oxide (GO). The quick removal of oxidized functional groups led to fast exfoliation of rGO. (Fig. 3) shows XRD patterns of Graphite, GO, rGO, and CU/rGO. The diffraction peak is at around angle 11.5, corresponding to the (001) rejection of GO. According to the Bragg equation, the calculated interplanar crystal spacing of GO is from 0.335 nm (pristine graphite powder) to 0.769 nm, which demonstrates that the GO has completely exfoliated. The oxygen-containing functional groups of GO could not be entirely eliminated by reducing elemental copper. Characteristic diffraction peaks of graphite oxide (001 and 002) at approximately 14° and 11.3°, respectively, remained in the XRD pattern of rGO film, besides a broad diffraction peak (002) of graphite at about 24°. The broadening and shift of the characteristic diffraction peak of graphite from 26.48° to 24° were due to the short-range order in stacked stacks.[38]

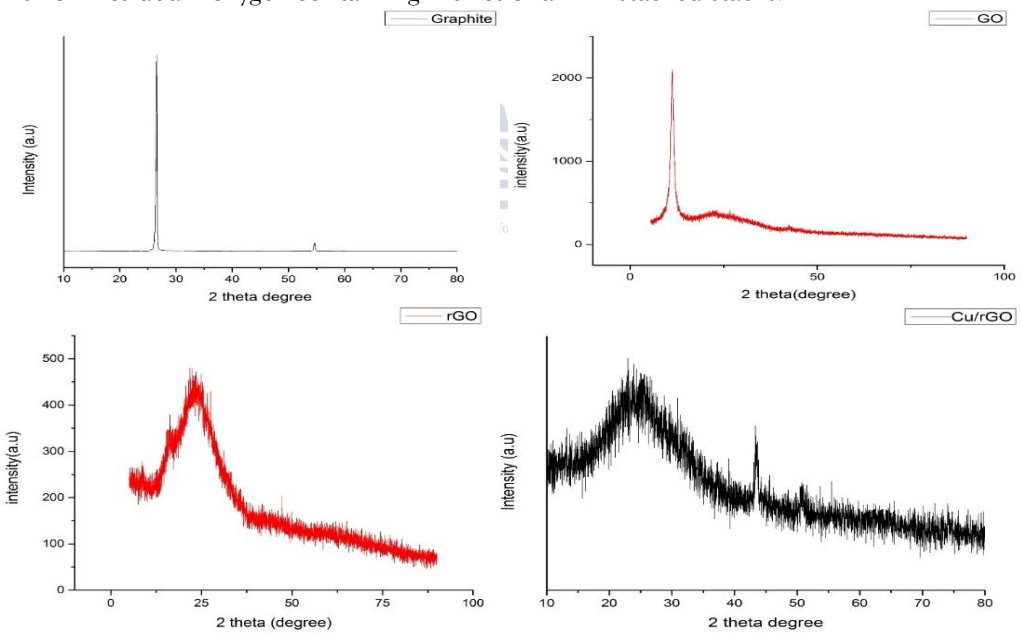

Figure 3 XRD pattern of a (a) Graphite, (b) Graphene oxide (GO), (c) reduced Graphene oxide (rGO) and (d) reduced Graphene oxide with large copper nanowires

Fourier Transform Infrared Spectroscopy (FTIR) Analysis:

The thick rGO films prepared with the immersion time of 1 h were peeled off from the copper substrate with tweezers and used for XRD and Fourier transform infrared spectroscopy (FT-IR) investigations. The reduction of Graphene Oxide to Reduced Graphene Oxide should result in structural change, especially in the distance between the layers. (Figure 4) shows FT-IR spectra of GO and rGO. The presence of different types of oxygen functionalities in GO was confirmed at 3,400 cm^{-1} (O–H-stretching vibrations), at 1,720 cm^{-1} (stretching vibrations from C=O), at 1,600 cm^{-1} (skeletal vibrations from unoxidized graphitic domains), at 1,220 cm^{-1} (C–OH-stretching vibrations), and at 1,060 cm^{-1} (C–O-stretching vibrations) [39]. FT-IR peak of RGO film presents that O–H-stretching vibrations observed at

3,400 cm^{-1} were significantly reduced due to deoxygenation. However, C–O-stretching vibrations at 1,060 cm^{-1} were still observed, caused by remaining carboxyl groups [40]. From the FT-IR and XRD characterisations of the produced rGO film, it can be concluded that elemental copper partially reduced the GO while some oxygen-containing groups remain. To improve its conductivity, the produced rGO needs to be further reduced.

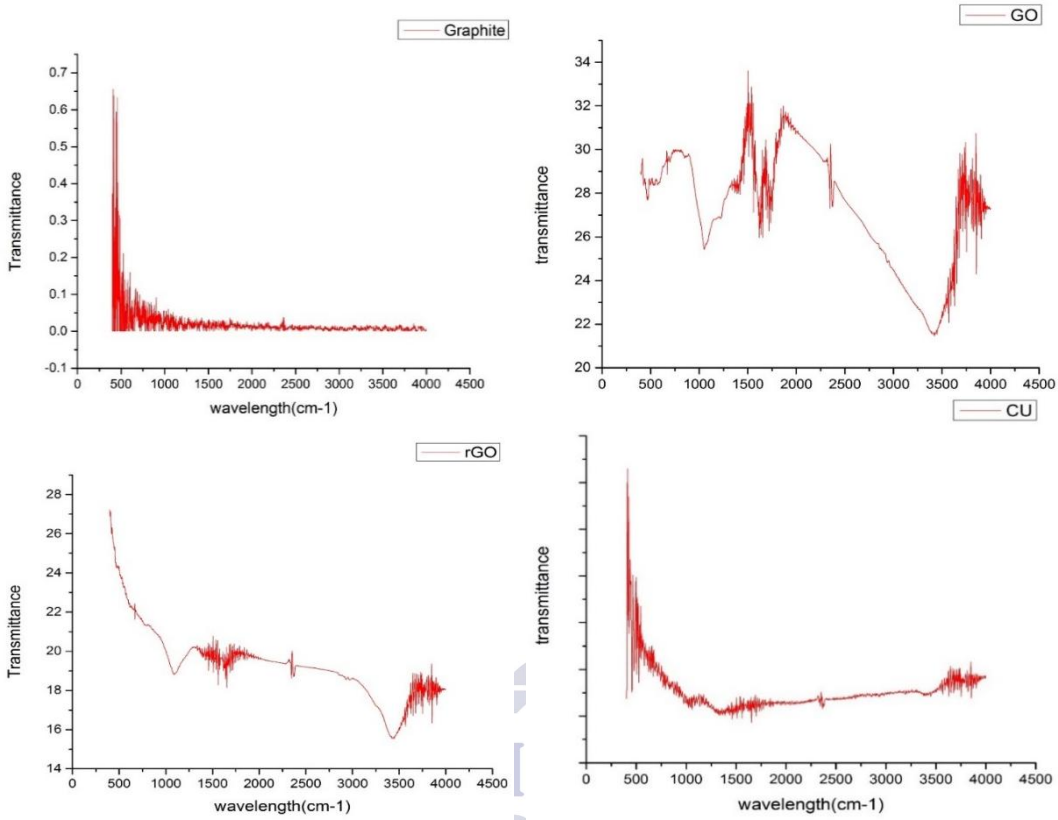

Figure 4 Fourier Transform Infrared Spectroscopy (FTIR) Analysis of (a) Graphite, (b) Graphene oxide (GO), (c) reduced Graphene oxide (rGO) and (D) Coppers

Raman Spectroscopy:

Raman spectra of graphite, rGO, rGO/CU SNWs and rGO/CU LNWs are shown in Fig. 5;

The Raman results are also consistent with the previous report.[41] After the reduction of GO, we notice two distinctive features which are related to the chemical reduction of GO. First, I(D)/I(G) of rGO is increased by some percentage, implying that small graphitic domains are formed after the reduction. In contrast, GO before the reduction is highly disordered to have small I(D)/I(G) to start with.[41] [42] Second, the increase of I(2D)/I(G) is observed, and this is another indication of graphitization. Raman spectra of graphite, GO, rGO, and rGO/Cu LNWs are shown in Fig. 5. A couple of Raman active bands can be observed for the pristine graphite. One is the G band at 1575 cm^{-1}; the other is the weak D band (defects inherent in the graphite and the edge effect of graphite, A1g mode) around 1350 cm^{-1}. The significant structure changed during the oxidation from graphite to GO; the G band was broadened and shifted to high frequency, and the D band became higher relative intensity. It reflected the reduction in the size of the in-plane sp^2 domains. When GO transformed to reduced graphene oxide, the G band slightly shifted back to the location of the G band in graphite. Meanwhile, the decrease of D band intensity was attributed to graphite by reduction.[43]

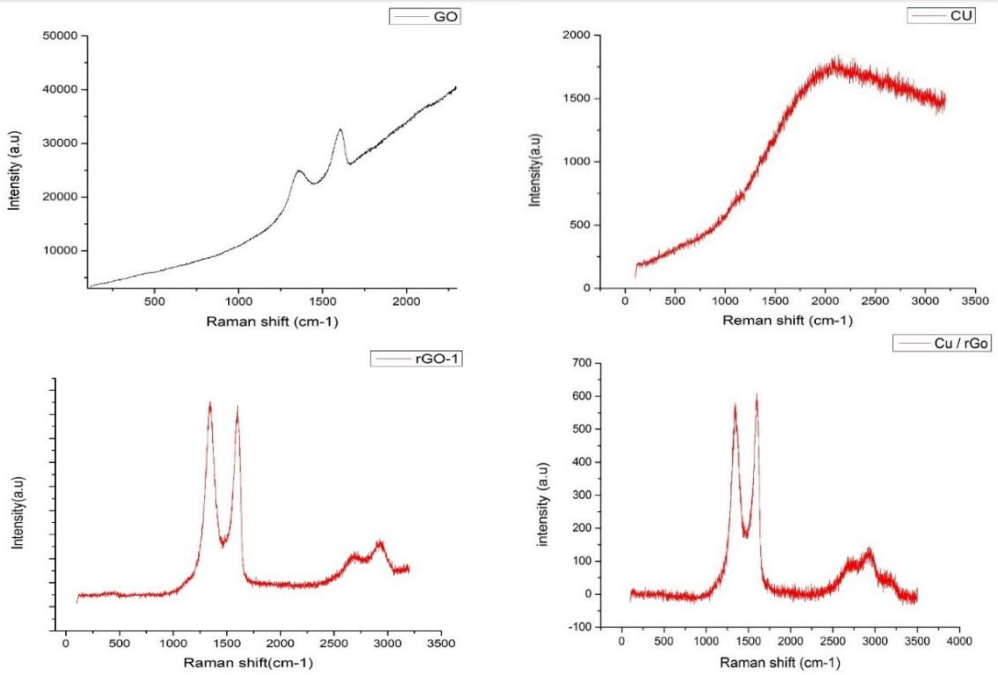

Figure 5 Raman Spectroscopy of (a) Graphene oxide, (b) Copper nanowires, (c) reduced Graphene oxide (rGO) and (d) rGO/ Cu LNWS respectively

Thermogravimetric analyser (TGA):

The first weight-loss stage below 250 °C is due to the decomposition of surface carboxyl or hydroxyl groups on GO.[44] For the thermally reduced GO sample, the weight loss below 250 °C is negligible, indicating the successful removal of the oxygen-related functional groups during the heat treatment. Another remarkable property of rGO paper is its high thermal stability, especially when compared with GO using thermogravimetric analysis (TGA) (Fig. 6). The mass loss below 200 C can be attributed to the evaporation of adsorbed water. A slight mass loss appears between 200 and 500 C, presumably owing to the decomposition of some residual oxygen-containing groups.

In contrast, to the GO paper (Fig. 6A), there is no sharp weight loss at around 200 C for the rGO paper, indicating that the hydrazine reduction has removed most oxygen-containing groups. The total weight loss (<10%) of graphene paper between 200 and 500 C is much lower than that of GO paper. When graphene paper is annealed between 200 and 500 C, the mechanical integrity of the paper, as well as the physical appearance (smooth, shiny surface), are retained. The lustrous appearance is enhanced by thermal annealing. These results clearly indicate that paper composed of chemically reduced graphene is much more thermally stable than unreduced GO paper.

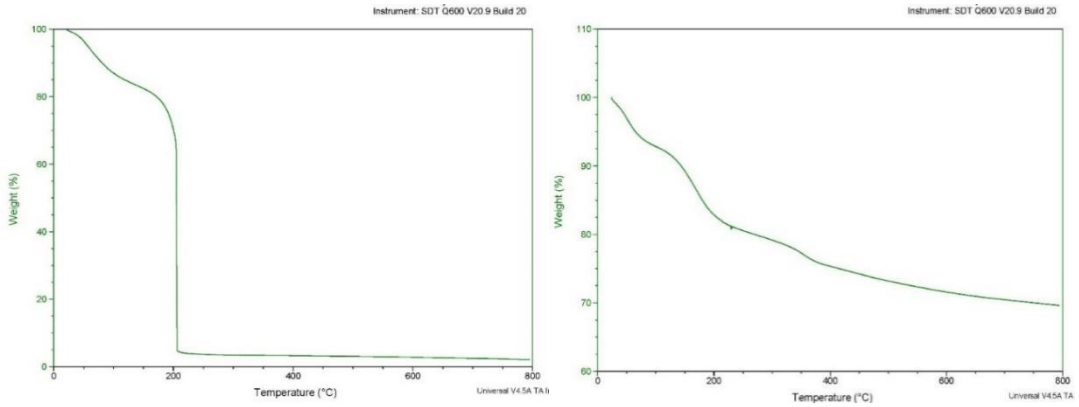

Figure 6 Thermogravimetric analyzer (TGA) of (a) Graphene oxide (GO) and (b) reduced Graphene oxide (rGO)

Measures the Electrical Conductivity:

The mechanical properties of the GO, rGO, and rGO/CU hybrid films were investigated by a tensile test, as shown in Fig. 7. Compared with GO, rGO, and rGO/CU hybrid films exhibit enhanced Young's modulus with a simultaneous slightly decrease in tensiles strength. The values are much larger than that of commercial flexible graphite paper (about 10 Mpa).[45] The electrical conductivity of the GO, rGO, and rGO/CU hybrid films was measured using the conductivity meter without additional annealing treatment. Fig. 8 shows high electrical conductivity (180 Ohms per sq), and the electrical conductivity of the prepared hybrid films significantly reduces from GO, which is all lower than that of rGO and rGO/CU films. The lowest sheet resistance is obtained from the rGO/CU hybrid film.

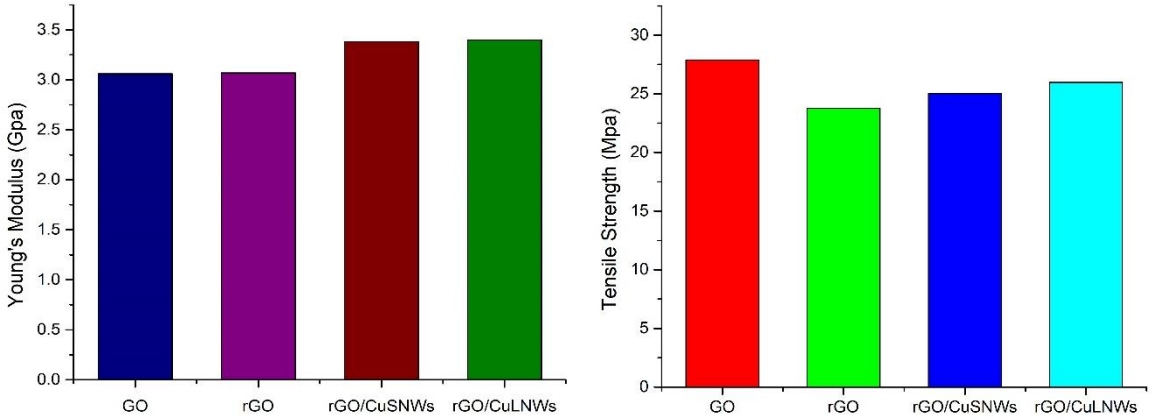

Fig. 7 Mechanical properties of GO, rGO and rGO/Cu NWS films for different mass ratio: (a) Young's modulus; (b) tensile strength.

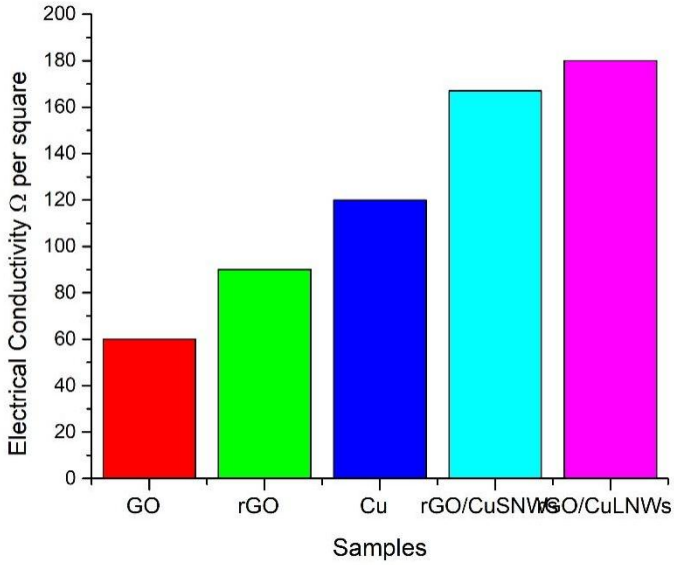

Fig. 8 Electrical Conductivity of GO, rGO, Cu, rGO/Cu SNWs and rGO/Cu LNWs composite film.

CONCLUSION

In summary, we have demonstrated a new solution-based approach to rGO nanosheets on the surface of ultrathin copper nanowires by mild Hydrazine hydrate. Both rGO/CU LNws and rGO/CU SNws hybrid free stand films were fabricated through vacuum-filtrating, controlled transferring and subsequent thermal reduction. As-made hybrid films, especially rGO/CU LNW hybrid films, exhibit good transparency and electrical conductivity, good oxidation resistance and thermal stability. It is mainly due to the correct combination of the electrical networks of CU NWs and the protective effect of the rGO over-coating layer. This work demonstrates a new approach to improving and stabilising ultrathin Graphene along metal nanowires. It takes one step further toward commercialising Graphene with copper nanowires as a low-cost transparent conductor for electrical conductivity applications.

AUTHOR INFORMATION

Corresponding Author

*E-mail: shahnawaz.phulpoto@sbbusba.edu.pk

Notes: The authors declare no competing financial interest.

Acknowledgement

This work was financially supported by the Higher Education Commission (HEC) Pakistan for Startup Research Grant Program (SRGP) (Grant No. 21-2123/SRGP/R&D/HEC/2018) in Shah Abdul Latif University Khairpur Sindh, Pakistan. The author would also like to thank the Shaheed Benazir Bhutto University, Shaheed Benazir Abad Sindh Pakistan. for their kind support in smoothly performing the research.

REFERENCES

1. Fan, X.; Peng, W.; Li, Y.; Li, X.; Wang, S.; Zhang, G.; Zhang, F., Deoxygenation of exfoliated graphite oxide under alkaline conditions: a green route to graphene preparation. *Advanced Materials* **2008,** *20* (23), 4490-4493.
2. (a) Novoselov, K. S.; Geim, A. K.; Morozov, S. V.; Jiang, D.-e.; Zhang, Y.; Dubonos, S. V.; Grigorieva, I. V.; Firsov, A. A., Electric field effect in atomically thin carbon films. *science* **2004,** *306* (5696), 666-669; (b) Phulpoto, S.; Memon, M. A.; Yan, S.; Geng, J., Macroporous graphene thin films as electrochemical electrodes: enhancing the sensitivity for detection of metal ions. *Journal of Nanoscience and Nanotechnology* **2018,** *18* (6), 4100-4105.
3. Stankovich, S.; Dikin, D. A.; Dommett, G. H.; Kohlhaas, K. M.; Zimney, E. J.; Stach, E. A.; Piner, R. D.; Nguyen, S. T.; Ruoff, R. S., Graphene-based composite materials. *nature* **2006,** *442* (7100), 282-286.
4. Dikin, D. A.; Stankovich, S.; Zimney, E. J.; Piner, R. D.; Dommett, G. H.; Evmenenko, G.; Nguyen, S. T.; Ruoff, R. S., Preparation and characterization of graphene oxide paper. *Nature* **2007,** *448* (7152), 457-460.
5. Li, D.; Kaner, R. B., Graphene-based materials. *Science* **2008,** *320* (5880), 1170-1171.
6. (a) Stankovich, S.; Dikin, D. A.; Piner, R. D.; Kohlhaas, K. A.; Kleinhammes, A.; Jia, Y.; Wu, Y.; Nguyen, S. T.; Ruoff, R. S., Synthesis of graphene-based nanosheets via chemical reduction of exfoliated graphite oxide. *carbon* **2007,** *45* (7), 1558-1565; (b) Stankovich, S.; Piner, R. D.; Chen, X.; Wu, N.; Nguyen, S. T.; Ruoff, R. S., Stable aqueous dispersions of graphitic nanoplatelets via the reduction of exfoliated graphite oxide in the presence of poly (sodium 4-styrenesulfonate). *Journal of Materials Chemistry* **2006,** *16* (2), 155-158.
7. McAllister, M. J.; Li, J.-L.; Adamson, D. H.; Schniepp, H. C.; Abdala, A. A.; Liu, J.; Herrera-Alonso, M.; Milius, D. L.; Car, R.; Prud'homme, R. K., Single sheet functionalized graphene by oxidation and thermal expansion of graphite. *Chemistry of materials* **2007,** *19* (18), 4396-4404.
8. Niyogi, S.; Bekyarova, E.; Itkis, M. E.; McWilliams, J. L.; Hamon, M. A.; Haddon, R. C., Solution properties of graphite and graphene. *Journal of the American Chemical Society* **2006,** *128* (24), 7720-7721.
9. Gilje, S.; Han, S.; Wang, M.; Wang, K. L.; Kaner, R. B., A chemical route to graphene for device applications. *Nano letters* **2007,** *7* (11), 3394-3398.
10. Gómez-Navarro, C.; Weitz, R. T.; Bittner, A. M.; Scolari, M.; Mews, A.; Burghard, M.; Kern, K., Electronic transport properties of individual chemically reduced graphene oxide sheets. *Nano letters* **2007,** *7* (11), 3499-3503.
11. Hsiao, S.-T.; Tien, H.-W.; Liao, W.-H.; Wang, Y.-S.; Li, S.-M.; MMa, C.-C.; Yu, Y.-H.; Chuang, W.-P., A highly electrically conductive graphene–silver nanowire hybrid nanomaterial for transparent conductive films. *Journal of materials chemistry C* **2014,** *2* (35), 7284-7291.
12. Geng, J.; Liu, L.; Yang, S. B.; Youn, S.-C.; Kim, D. W.; Lee, J.-S.; Choi, J.-K.; Jung, H.-T., A simple approach for preparing transparent conductive graphene films using the controlled chemical reduction of exfoliated graphene oxide in an aqueous suspension. *The Journal of Physical Chemistry C* **2010,** *114* (34), 14433-14440.
13. Memon, M. A.; Bai, W.; Sun, J.; Imran, M.; Phulpoto, S. N.; Yan, S.; Huang, Y.; Geng, J., Conjunction of conducting polymer nanostructures with macroporous structured graphene thin films for high-performance flexible supercapacitors. *ACS applied materials & interfaces* **2016,** *8* (18), 11711-11719.
14. Xue, J.; BinAhmed, S.; Wang, Z.; Karp, N. G.; Stottrup, B. L.; Romero-Vargas Castrillón, S., Bacterial adhesion to graphene oxide (GO)-functionalized interfaces is determined by hydrophobicity and GO sheet spatial orientation. *Environmental Science & Technology Letters* **2018,** *5* (1), 14-19.
15. Li, H.; Pang, S.; Wu, S.; Feng, X.; Müllen, K.; Bubeck, C., Layer-by-layer assembly and UV photoreduction of graphene–polyoxometalate composite films for electronics. *Journal of the*

American Chemical Society **2011,** *133* (24), 9423-9429.
16. Wu, H.; Hu, L.; Rowell, M. W.; Kong, D.; Cha, J. J.; McDonough, J. R.; Zhu, J.; Yang, Y.; McGehee, M. D.; Cui, Y., Electrospun metal nanofiber webs as high-performance transparent electrode. *Nano letters* **2010,** *10* (10), 4242-4248.
17. Lu, L.; Shen, Y.; Chen, X.; Qian, L.; Lu, K., Ultrahigh strength and high electrical conductivity in copper. *Science* **2004,** *304* (5669), 422-426.
18. Wang, S.; Cheng, Y.; Wang, R.; Sun, J.; Gao, L., Highly thermal conductive copper nanowire composites with ultralow loading: toward applications as thermal interface materials. *ACS applied materials & interfaces* **2014,** *6* (9), 6481-6486.
19. Kudo, H.; Fujihira, M., DNA-templated copper nanowire fabrication by a two-step process involving electroless metallization. *IEEE transactions on nanotechnology* **2006,** *5* (2), 90-92.
20. Lisiecki, I.; Pileni, M., Synthesis of well-defined and low size distribution cobalt nanocrystals: the limited influence of reverse micelles. *Langmuir* **2003,** *19* (22), 9486-9489.
21. Mohl, M.; Pusztai, P.; Kukovecz, A.; Konya, Z.; Kukkola, J.; Kordas, K.; Vajtai, R.; Ajayan, P. M., Low-temperature large-scale synthesis and electrical testing of ultralong copper nanowires. *Langmuir* **2010,** *26* (21), 16496-16502.
22. Zhang, X.; Yan, X.; Chen, J.; Zhao, J., Large-size graphene microsheets as a protective layer for transparent conductive silver nanowire film heaters. *Carbon* **2014,** *69*, 437-443.
23. Huang, S.-Y.; Zhang, K.; Yuen, M. M.; Fu, X.-Z.; Sun, R.; Wong, C.-P., Facile synthesis of flexible graphene–silver composite papers with promising electrical and thermal conductivity performances. *Rsc Advances* **2014,** *4* (64), 34156-34160.
24. Berman, R.; Macdonald, D. K. C., The thermal and electrical conductivity of copper at low temperatures. *Proceedings of the Royal Society of London. Series A. Mathematical and Physical Sciences* **1952,** *211* (1104), 122-128.
25. Kevin, M.; Ong, W.; Lee, G.; Ho, G., Formation of hybrid structures: copper oxide nanocrystals templated on ultralong copper nanowires for open network sensing at room temperature. *Nanotechnology* **2011,** *22* (23), 235701.
26. Wang, R.; Ruan, H., Synthesis of copper nanowires and its application to flexible transparent electrode. *Journal of Alloys and Compounds* **2016,** *656*, 936-943.
27. Iqbal, M.; Thebo, A. A.; Shah, A. H.; Iqbal, A.; Thebo, K. H.; Phulpoto, S.; Mohsin, M. A., Influence of Mn-doping on the photocatalytic and solar cell efficiency of CuO nanowires. *Inorganic Chemistry Communications* **2017,** *76*, 71-76.
28. Iqbal, M.; Ali, A.; Nahyoon, N. A.; Majeed, A.; Pothu, R.; Phulpoto, S.; Thebo, K. H., Photocatalytic degradation of organic pollutant with nanosized cadmium sulfide. *Materials Science for Energy Technologies* **2019,** *2* (1), 41-45.
29. Thebo, A. A.; Nahyoon, N. A.; Phulpoto, S. N.; Khan, A.; Shah, S. A.; Ali, S.; Thebo, K. H., Synthesis, Characterization and Biological Evaluation of Copper (ii) Metal Complex with 1, 10-Phenanthroline. *Organic & Medicinal Chemistry International Journal* **2017,** *2* (1), 8-12.
30. Phulpoto, S.; Sun, J.; Qi, S.; Xiao, L.; Yan, S.; Geng, J., Tuning the morphologies of fluorine-doped tin oxides in the three-dimensional architecture of graphene for high-performance lithium-ion batteries. *Nanotechnology* **2017,** *28* (39), 395404.
31. Li, Y.; Chen, H.; Voo, L. Y.; Ji, J.; Zhang, G.; Zhang, G.; Zhang, F.; Fan, X., Synthesis of partially hydrogenated graphene and brominated graphene. *Journal of Materials Chemistry* **2012,** *22* (30), 15021-15024.
32. Xu, C.; Wang, X.; Zhu, J., Graphene− metal particle nanocomposites. *The Journal of Physical Chemistry C* **2008,** *112* (50), 19841-19845.
33. Ali, A.; Pothu, R.; Siyal, S. H.; Phulpoto, S.; Sajjad, M.; Thebo, K. H., Graphene-based membranes for CO2 separation. *Materials Science for Energy Technologies* **2019,** *2* (1), 83-88.
34. Mani, V.; Periasamy, A. P.; Chen, S.-M., Highly selective amperometric nitrite sensor based on chemically reduced graphene oxide modified electrode. *Electrochemistry Communications* **2012,** *17*, 75-78.
35. Wang, X.; Zhi, L.; Tsao, N.; Tomović, Ž.; Li, J.; Müllen, K., Transparent carbon films as electrodes in organic solar cells. *Angewandte Chemie International Edition* **2008,** *47* (16), 2990-2992.
36. Bello, A.; Fabiane, M.; Momodu, D. Y.; Khamlich, S.; Dangbegnon, J. K.; Manyala, N., Functionalized graphene foam as electrode for

improved electrochemical storage. *Journal of Solid State Electrochemistry* **2014,** *18* (9), 2359-2365.
37. Lu, C. H.; Yang, H. H.; Zhu, C. L.; Chen, X.; Chen, G. N., A graphene platform for sensing biomolecules. *Angewandte Chemie* **2009,** *121* (26), 4879-4881.
38. Becerril, H. A.; Mao, J.; Liu, Z.; Stoltenberg, R. M.; Bao, Z.; Chen, Y., Evaluation of solution-processed reduced graphene oxide films as transparent conductors. *ACS nano* **2008,** *2* (3), 463-470.
39. Eda, G.; Fanchini, G.; Chhowalla, M., Large-area ultrathin films of reduced graphene oxide as a transparent and flexible electronic material. *Nature nanotechnology* **2008,** *3* (5), 270-274.
40. Zhou, X.; Huang, X.; Qi, X.; Wu, S.; Xue, C.; Boey, F. Y.; Yan, Q.; Chen, P.; Zhang, H., In situ synthesis of metal nanoparticles on single-layer graphene oxide and reduced graphene oxide surfaces. *The Journal of Physical Chemistry C* **2009,** *113* (25), 10842-10846.
41. Berger, C.; Song, Z.; Li, T.; Li, X.; Ogbazghi, A. Y.; Feng, R.; Dai, Z.; Marchenkov, A. N.; Conrad, E. H.; First, P. N., Ultrathin epitaxial graphite: 2D electron gas properties and a route toward graphene-based nanoelectronics. *The Journal of Physical Chemistry B* **2004,** *108* (52), 19912-19916.
42. Berger, C.; Song, Z.; Li, X.; Wu, X.; Brown, N.; Naud, C.; Mayou, D.; Li, T.; Hass, J.; Marchenkov, A. N., Electronic confinement and coherence in patterned epitaxial graphene. *Science* **2006,** *312* (5777), 1191-1196.
43. Kim, K. S.; Zhao, Y.; Jang, H.; Lee, S. Y.; Kim, J. M.; Kim, K. S.; Ahn, J.-H.; Kim, P.; Choi, J.-Y.; Hong, B. H., Large-scale pattern growth of graphene films for stretchable transparent electrodes. *nature* **2009,** *457* (7230), 706-710.
44. Reina, A.; Jia, X.; Ho, J.; Nezich, D.; Son, H.; Bulovic, V.; Dresselhaus, M. S.; Kong, J., Large area, few-layer graphene films on arbitrary substrates by chemical vapor deposition. *Nano letters* **2009,** *9* (1), 30-35.
45. Wei, X. H.; Liu, L.; Zhang, J. X.; Shi, J. L.; Guo, Q. G., Mechanical, electrical, thermal performances and structure characteristics of flexible graphite sheets. *Journal of materials science* **2010,** *45* (9), 2449-2455.